# Mechanism of Myosin Subfragment-1-Induced Assembly of CaG-Actin and MgG-Actin into F-Actin−$S_1$-Decorated Filaments†

Stéphane Fievez, Marie-France Carlier,* and Dominique Pantaloni

*Laboratoire d'Enzymologie et Biochimie Structurales, CNRS, 91198 Gif-sur-Yvette, France*

*Received May 22, 1997; Revised Manuscript Received July 22, 1997*⊗

ABSTRACT: The kinetics and mechanism of myosin subfragment-1-induced polymerization of G-actin into F-actin−$S_1$-decorated filaments have been investigated in low ionic strength buffer and in the absence of free ATP. The mechanism of assembly of F-actin−$S_1$ differs from salt-induced assembly of F-actin. Initial condensation of G-actin and $S_1$ into oligomers in reversible equilibrium is a prerequisite step in the formation of F-actin−$S_1$ . Oligomers have a relatively low stability ($10^6$ $M^{-1}$) and contain $S_1$ in a molar ratio to actin close to 0.5. Increased binding of $S_1$ up to a 1:1 molar ratio to actin is associated with further irreversible condensation of oligomers into large F-actin−$S_1$ structures of very high stability. In contrast to salt-induced assembly of F-actin, no monomer−polymer equilibrium, characterized by a critical concentration, can be defined for F-actin−$S_1$ assembly, and end-to-end annealing of oligomers is predominant over growth from nuclei in the kinetics. Simultaneous recordings of the changes in light scattering, pyrenyl- and NBD-actin fluorescence, ATP hydrolysis, and release of $P_i$ during the polymerization process have been analyzed to propose a minimum kinetic scheme for assembly, within which several elementary steps, following oligomer formation, are required for assembly of F-actin−$S_1$. ATP hydrolysis occurs before polymerization of MgATP−G-actin but not of CaATP−G-actin. The release of inorganic phosphate occurs on F-actin−$S_1$ at the same rate as on F-actin.

In low ionic strength buffers, in which repulsive interactions maintain actin itself in its monomeric (G-actin) form, the myosin head (myosin subfragment-1, $S_1$) induces the assembly of F-actin−$S_1$-decorated filaments (*1*−*7*). The product of the assembly reaction is biochemically and structurally indistinguishable from the standard arrowhead-decorated filaments obtained by binding $S_1$ to preassembled F-actin thin filaments in the absence of ATP (*6*). The actin−actin interactions in the polymer assembled by combining G-actin and $S_1$ are typical actin−actin bonds in the filaments, and the actin:$S_1$ molar ratio is 1:1.

Previous studies (*6*) suggested that the formation of F-actin−$S_1$ did not obey the standard nucleation-growth kinetic scheme known to account for salt-induced polymerization of G-actin into F-actin. Rather, the self-association of G-actin−$S_1$ complexes seemed to account for the sharp transition in light scattering measurements observed at a 1:1 actin−$S_1$ molar ratio. The evidence for the initial rapid formation of binary G-S and ternary $G_2S$ complexes as first kinetic intermediates in the polymerization process (*8*, *9*) as well as their subsequent self-condensation into oligomers, precursors of F-actin−$S_1$ (*10*, *22*) is supportive of such a process. An opposite view, within which assembly of F-actin−$S_1$ would proceed via nucleation and growth, has been expressed (*7*).

The kinetics of $S_1$-induced polymerization of G-actin has been examined using a combination of light-scattering intensity and the fluorescence changes of pyrenyl- and NBD-labeled actin as probes. The hydrolysis of ATP and the release of $P_i$ during formation of F-actin−$S_1$ have also been monitored. Kinetic global analysis of these different processes leads to a minimum model describing the mechanism of assembly. Experiments have been performed with the $S_1(A_1)$ and $S_1(A_2)$ isoforms of $S_1$ (carrying either the $A_1$ or the $A_2$ essential light chain), and emphasis has been brought on the role of the divalent metal ion ($Ca^{2+}$ or $Mg^{2+}$) tightly bound to actin in association with ATP.

## MATERIALS AND METHODS

*Chemicals.* Pyrenyl iodoacetamide was from Molecular Probes, NBD-Cl from Aldrich, α-chymotrypsin from Worthington, and γ-[$^{32}$P]-ATP from Amersham. All other chemicals were of analytical grade.

*Proteins.* The procedures for purification of G-actin from rabbit muscle, fluorescent pyrenyl- or NBD-labeling of actin and $Ca^{++}/Mg^{++}$ exchange are all described by Fievez *et al*. (*22*). γ-[$^{32}$P]-ATP−G-actin 1:1 complex was prepared by incubating CaATP−G-actin in G buffer with γ-[$^{32}$P]-ATP overnight at 0 °C prior to Dowex-1 treatment.

Preparation of myosin and the isoforms of subfragment-1 was performed as described by Fievez *et al*. (*22*).

Protein concentrations were determined spectrophotometrically (*10*).

*Light Scattering and Fluorescence Measurements.* The time course of formation of F-actin−$S_1$ decorated filaments was monitored by light scattering at 90° angle and at a wavelength of 400 nm, using a Spex Fluorolog2 spectrofluorimeter thermostated at 20 °C. The polymerization reaction was started by adding $S_1(A_1)$ or $S_1(A_2)$ to either CaATP−G-actin or MgATP−G-actin 1:1 complex in low ionic strength $G_0$ buffer (buffer G without ATP, which was

† This work was supported in part by the Association Française contre les Myopathies (AFM), the Ligue Nationale Française contre le Cancer, the Association pour la Recherche contre le Cancer (ARC), and an EEC Grant CHRX-CT94-0652.

* Corresponding author. Tel. 01 69 82 34 65. Fax: 01 69 82 31 29. E-mail: carlier@lebs.cnrs-gif.fr.

⊗ Abstract published in *Advance ACS Abstracts,* September 15, 1997.

S0006-2960(97)01206-3 CCC: $14.00 

supplemented with 0.2 mM EGTA and 10 $\mu$M $MgCl_2$ for experiments with MgATP−G-actin).

The changes in fluorescence of pyrenyl-actin or NBD-actin associated to the assembly of F-actin−$S_1$ were monitored under the same conditions, with excitation wavelengths of 366 and 475 nm and emission wavelengths of 387 and 530 nm for pyrenyl and NBD fluorescence, respectively.

*ATPase Measurements.* The formation of acid-labile $P_i$ resulting from the chemical cleavage of the $\gamma$-phosphate of actin-bound $\gamma$-[$^{32}$P]-ATP during assembly of decorated filaments was measured by extraction of the [$^{32}$P]-labeled phosphomolybdate complex (*11*). The release of $P_i$ in the medium was monitored spectrophotometrically at 360 nm using the MESG/purine phosphorylase as an enzyme-linked assay (*12*, *13*).

## RESULTS

*$S_1$-Induced Polymerization of G-Actin into F-Actin−$S_1$-Decorated Filaments Is Not Characterized by a Critical Concentration.* The spontaneous polymerization of G-actin into filaments, induced by an increase in ionic strength, is known to be a nucleated-growth process, similar to the crystallization of a solute, and is characterized by the existence of a critical concentration for assembly. The critical concentration is the concentration of monomeric (G-) actin which coexists with F-actin filaments at steady state in the presence of ATP (or at equilibrium in the presence of ADP) and maintains the stability of the polymer via monomer−polymer exchange reactions at the ends. The value of the critical concentration for F-actin assembly can be estimated as the abscissa intercept of the plots of the mass amount of F-actin present at steady state at different concentrations of total actin. Identical critical concentration plots of F-actin vs total actin are routinely obtained when actin is assembled at different concentrations and when actin is assembled at a high concentration, then serially diluted to different concentrations in polymerization buffer.

To determine whether the assembly of F-actin−$S_1$-decorated filaments is characterized by a critical concentration, CaATP−G-actin (12 $\mu$M) 1:1 complex in $G_0$ buffer was assembled into F-actin−$S_1$ by addition of 18 $\mu$M $S_1(A_2)$, then diluted to different concentrations in $G_0$ buffer. Parallel samples were prepared in which CaATP−G-actin at different concentrations (0−12 $\mu$M) in $G_0$ buffer was mixed with 1.5 M equiv $S_1(A_2)$. The intensity of scattered light was measured after overnight incubation of the two series of samples. Data displayed in Figure 1 show that in a range of high enough actin concentrations ($\geq$6 $\mu$M) identical values of light scattering intensity were measured for the pair of samples which contained the same amounts of actin and $S_1$, but had been processed in two different fashions. At lower actin concentration, however, different readings were obtained for the two series of samples. Data points corresponding to samples obtained by serial dilution of the concentrated F-actin−$S_1$ solution fell on a line passing through the origin. The points deviated from linearity at high actin and $S_1$ concentrations, due to the nonideality of the solution and the intervening of the second viriel coefficient (*14*). The absence of critical concentration was validated by fluorescence measurements of serially diluted samples of pyrenyl-F-actin−$S_1$ (Figure 1, inset). In contrast, data points corresponding to samples in which actin was

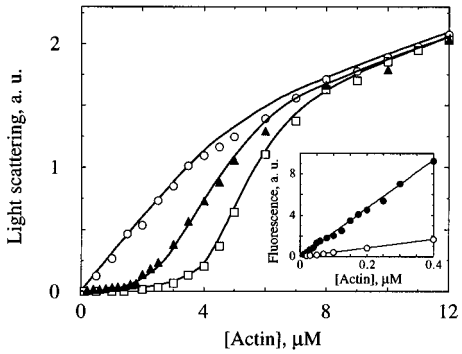


FIGURE 1: Change in light scattering upon assembly of F-actin−$S_1$ from $S_1(A_2)$ and CaATP−G-actin or MgATP−G-actin. CaATP−G-actin (□) or MgATP−G-actin (▲) 1:1 complex at the indicated concentrations was combined with 1.5 M equiv $S_1(A_2)$ in $G_0$ buffer. Light scattering at 90° angle was measured at 400 nm on each sample after 18 h incubation. Alternatively, CaATP−G-actin (12 $\mu$M) was premixed with 18 $\mu$M $S_1(A_2)$, incubated for 15 min until assembly of F-actin−$S_1$ was complete, then diluted to the indicated concentrations (○) in $G_0$ buffer and incubated for 18 h before the light scattering measurements were made. (Inset) Samples prepared from pyrenyl-labeled actin (85% labeled) were processed as in main panel (○), but pyrenyl fluorescence was measured in a low concentration range. (●) F-actin−$S_1$ serially diluted samples. (○) Fluorescence of G-actin at the same concentration.

assembled, at each concentration, by addition of 1.5 M amount of $S_1$ yielded a sigmoidal spoon-shaped curve. The sigmoidicity was more pronounced with Ca-actin than with Mg-actin. Measurements carried out after incubation periods longer than 18 h yielded values identical to those shown in Figure 1.

To understand whether the failure of the mixture of Ca-G-actin and $S_1(A_2)$ to spontaneously polymerize at low actin concentration (<3 $\mu$M) was due to a highly unfavorable nucleation step, a solution of 2 $\mu$M Ca-G-actin and 3 $\mu$M $S_1(A_2)$ was supplemented with 2% (v/v) of a preassembled F-actin−$S_1$ solution (12 $\mu$M) as seeds. A very slow increase in NBD fluorescence was observed over a period of 30 min. In contrast, when the same F-actin−$S_1$ seeds were added to 2 $\mu$M Ca-G-actin alone in buffer $G_0$ supplemented with 0.1 M KCl, active seeded polymerization was observed, with an initial rate 25-fold higher than the rate measured for F-actin−$S_1$ elongation, indicating that the association rate constant of GS and/or $G_2S$ to F-actin−$S_1$ is 25-fold lower than the rate constant for association of Ca-actin to filaments (*11*), i.e., $k_+ = 5/25\ \mu M^{-1}\ s^{-1} = 0.2\ \mu M^{-1}\ s^{-1}$.

In another experiment, shown in Figure 2, G-actin (8 $\mu$M) was polymerized by addition of 23 $\mu$M $S_1(A_2)$. As soon as the light scattering plateau was reached ($t$ = 220 s), G-actin was added in a range of concentrations below the threshold concentration for spontaneous assembly of F-actin−$S_1$. An immediate increase in light scattering was observed. The process was first order, with a rate constant $k_{obs} = 0.04\ s^{-1}$, independent of the actin concentration. The extent of increase in light scattering was consistent with the incorporation of all the added actin subunits into F-actin−$S_1$. Examination of the late stages of spontaneous assembly of 8 $\mu$M G-actin by $S_1$ (main curve in Figure 2) shows that the rate of polymerization was 2.5-fold higher at time 40 s, at which 3 $\mu$M actin remained to be assembled, than when 3 $\mu$M actin was added at time 220 s. When 3 $\mu$M G-actin was added to the same preassembled F-actin−$S_1$ solution after 90 min of polymerization, the rate of increase in light

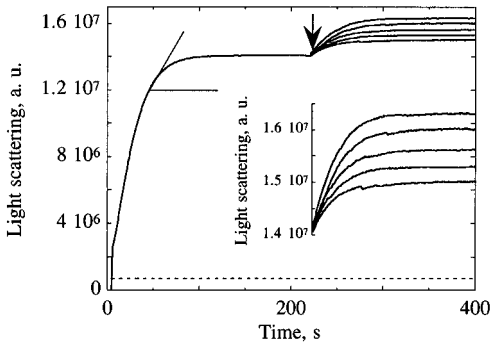


FIGURE 2: G-actin−$S_1$ complexes associate slowly to the ends of F-actin−$S_1$ filaments. CaATP−G-actin (8 $\mu$M) was polymerized by addition of 23 $\mu$M $S_1(A_2)$. At time 220 s (arrow), CaATP−G-actin at 3.0, 2.5, 2.0, 1.5, and 1.0 $\mu$M (top to bottom) was added to the solution. The change in light scattering at 400 nm was recorded. An expansion of the growth process is shown. Note that the rate of polymerization of 3 $\mu$M actin added at time 220 s is 2.5-fold lower than the rate measured in the main curve at time 40 s (light line tangent to the curve), at which 3 $\mu$M actin remain unassembled. The dashed line is the recorded light scattering of a sample containing 3 $\mu$M CaATP−G-actin and supplemented with 6 $\mu$M $S_1(A_2)$ at time zero.

scattering was 3-fold lower than when it was added at time 220 s. These results indicate that the GS and $G_2S$ complexes can associate in an endwise fashion to preassembled F-actin−$S_1$ filaments, but the number of sites available for elongation decreases during polymerization, most likely as a result of rapid annealing of short polymers. The value of $k_{obs} = 0.04$ $s^{-1}$ represents the product of the concentration of elongation sites at time 220 s by the association rate constant $k_+ = 0.2$ $\mu M^{-1}$ $s^{-1}$ of GS and/or $G_2S$ to F-actin−$S_1$. The concentration of F-actin−$S_1$ ends at time 220 s was 0.04/0.2 = 0.2 $\mu$M, that is about 2 orders of magnitude higher than the typical concentration of filaments in salt-induced spontaneous assembly of F-actin.

The apparent threshold concentration above which F-actin−$S_1$ can be assembled (Figure 1) cannot be considered as a critical concentration. Rather the results suggest that some reaction, highly dependent on actin concentration, is rate-limiting in the process of assembly of F-actin−$S_1$, but once started, the assembly of F-actin−$S_1$ proceeds irreversibly to completion until all actin subunits are incorporated in the polymer. At the end of the assembly process, neither monomeric actin nor G-actin−$S_1$ complex at the threshold concentration of 3 $\mu$M exists in equilibrium with F-actin−$S_1$. Sedimentation of the F-actin−$S_1$ samples followed by SDS−PAGE of the supernatants confirmed the absence of unpolymerized actin.

In conclusion, the mechanism of $S_1$-induced polymerization of actin into F-actin−$S_1$ appears different from polymerization of F-actin induced by salt. In the latter process, the concentration of nuclei formed initially is 3−4 orders of magnitude lower than the monomer concentration, and growth of the polymer essentially occurs via monomer association to these nuclei. At equilibrium, F-actin coexists with G-actin at the critical concentration. In contrast, nucleation of many short polymers is favored by $S_1$. These polymers grow both by end-to-end isodesmic association and endwise elongation, the elongation process being much slower than elongation of F-actin in the presence of salt, and not faster than the rate of end-to-end annealing of short polymers.

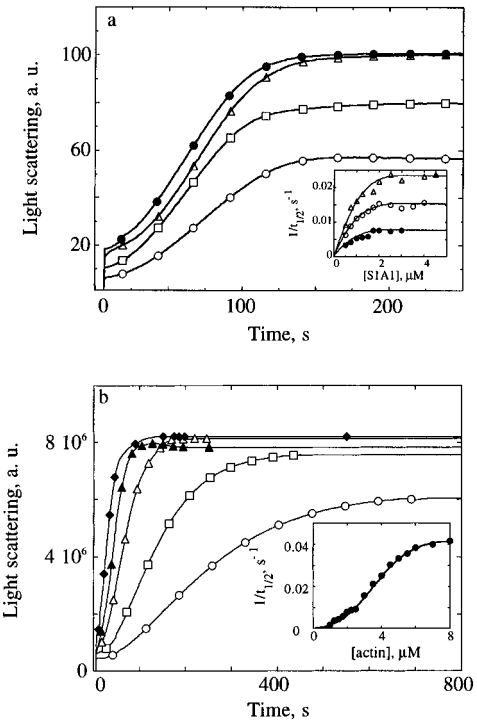


FIGURE 3: Kinetics of F-actin−$S_1$ assembly monitored by light scattering. (A) Dependence on $S_1$ concentration. CaATP−G-actin (3 $\mu$M) was combined with $S_1(A_1)$ at the following concentrations, in micromolar: 1.5 (○); 2 (□); 3 (△); 4 (●). (Inset) Dependence of the reciprocal of the half-polymerization time on $S_1$ concentration, at 2 (●); 3 (○) and 4 (△) $\mu$M G-actin. (B) Dependence on G-actin concentration. $S_1(A_1)$ (2 $\mu$M) was combined with CaATP−G-actin at the following concentrations, in micromolar: 1.5 (○); 2.0 (□); 3.0 (△); 4.5 (▲); 6.0 (■). (Inset) The reciprocal of the half-polymerization time is plotted versus the concentration of G-actin, at 2 $\mu$M $S_1$.

*Kinetics of F-Actin−$S_1$ Assembly Exhibit Different Dependences on G-Actin and $S_1$ Concentrations.* The time course of $S_1$-induced assembly of CaATP−G-actin 1:1 complex into F-actin−$S_1$ was monitored by the increase in light scattering, either at constant G-actin concentration and varying $S_1$ (Figure 3a) or at constant $S_1$ and varying G-actin (Figure 3b). The change in intensity of scattered light showed a small instantaneous increase upon addition of $S_1$ to G-actin, followed by a short lag preceding the large increase in light scattering which represented the formation of F-actin−$S_1$ proper. The duration of the lag was a decreasing function of both $S_1$ and G-actin concentration; however, it reached a finite lower limit at very high concentrations of $S_1$ and G-actin. The nature of the elementary steps taking place prior to the large increase in light scattering will be identified later on in the paper using the fluorescence of pyrenyl-actin or NBD-actin as more sensitive probes. The polymerization process that developed after the lag could not be described by an exponential, indicating that it did not consist in a simple growth of polymers maintained at a constant concentration, in agreement with data in the previous section.

When G-actin concentration was maintained constant, the rate of F-actin−$S_1$ assembly increased with $S_1$ concentration and reached a maximum value at an $S_1$:G-actin molar ratio lower than 1 (Figure 3a, inset). On the other hand, in agreement with a previous report (*5*), the extent of change in light scattering reached at the end of the polymerization process increased linearly with $S_1$ and reached a maximum

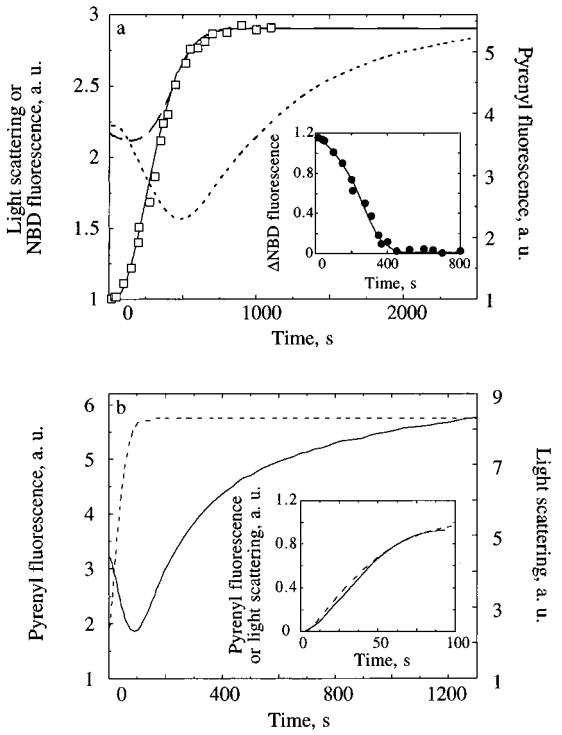


FIGURE 4: Simultaneous changes in light scattering, pyrenyl-actin, and NBD-actin fluorescences during assembly of Ca-F-actin−$S_1$. (A) CaATP−G-actin (2.0 $\mu$M, containing 20% pyrenyl-labeled and 15% NBD-labeled actin) was combined with 3 $\mu$M $S_1(A_1)$ at time zero. The time courses of changes in light scattering intensity (solid line), NBD fluorescence (dashed line), and pyrenyl-fluorescence (dotted line) were recorded at 400 nm on three parallel samples. (Open circles) Contribution of the irreversible assembly of F-actin−$S_1$ in the overall (dashed line) NBD fluorescence change. Samples were diluted 8-fold at the indicated times, NBD fluorescence was measured immediately following dilution and mutliplied by 8. The curve described by the open circles superimposes the light scattering change. The inset represents the difference between the overall NBD fluorescence curve (dashed) and the curve described by open circles, hence represents the time-dependent change in NBD fluorescence associated to a kinetic step preceding the assembly of F-actin−$S_1$. (B) Temporal correlation between the initial decrease in pyrenyl-actin fluorescence and the increase in light scattering. CaATP−G-actin (10 $\mu$M, 80% pyrenyl-labeled) was combined with 5 $\mu$M $S_1(A_1)$. The increase in light scattering at 600 nm (dashed line) and the change in pyrenyl fluorescence (solid line) were recorded on parallel samples. (Inset) The relative increase in light scattering and decrease in pyrenyl fluorescence in the time interval 0−100 s were normalized and are shown to be superimposable.

at an $S_1$:G-actin ratio of 1. Accordingly, when $S_1$ was kept at a constant concentration, the rate of F-actin−$S_1$ assembly continued to increase with actin concentration, above the 1:1 molar ratio to $S_1$ at which the maximum extent of increase in light scattering was reached (Figure 3b, inset).

In conclusion, although the actin:$S_1$ molar ratio is 1:1 in the final product of the reaction, the two components $S_1$ and actin do not play interchangeable roles in the kinetic pathway. These kinetic data are consistent with the view that the condensation of $G_2S$ and GS complexes into oligomers is required for F-actin−$S_1$ assembly.

*Correlation between the Changes in Light Scattering, Pyrenyl-Actin, and NBD-Actin Fluorescence during Assembly of F-Actin−$S_1$.* In a typical experiment, CaATP−G-actin (2 $\mu$M, 20% pyrenyl labeled, 15% NBD-labeled) was polymerized by addition of 3 $\mu$M $S_1(A_1)$. The recorded simultaneous changes in light scattering, pyrenyl, and NBD fluorescences are shown in Figure 4a. Upon addition of $S_1$,

Table 1: Light Scattering and Labeled Actin Fluorescence Parameters Associated to the Different Kinetic Intermediates in F-Actin−$S_1$ Assembly from ATP−G-Actin and $S_1$[a]

| species | LS[a] | NBD fluorescence | pyrenyl fluorescence |
|---|---|---|---|
| G-actin | <<1 | 1 | 1 |
| GS, $G_2S$ | <<1 | 1 | 3 |
| $G_iS$ oligomers | 1 | 2.2 | 4 |
| $(AS)_n$ oligomers | 1 | 1 | 4 |
| F-ADP-$P_iS_1$ | 6 | 2.9 | 1.5 |
| F-ADP-$S_1$ | 6 | 2.9 | 6 |

[a] A reference value of 1 is arbitrarily attributed to the specific light scattering of G-actin−$S_1$ oligomers and to the pyrenyl and NBD fluorescences of G-actin. LS, light scattering.

the small instantaneous increase in light scattering was linked to 3.8- and 2.1-fold increases in the fluorescence of pyrenyl- and NBD-actin respectively (Table 1). These rapid reactions, which are completed within the 5 s mixing time, reflect the formation and condensation of GS and $G_2S$ complexes into G-actin−$S_1$ oligomers in rapid equilibrium. The change in pyrene fluorescence mainly reflects the formation of GS and $G_2S$, while the change in NBD fluorescence specifically monitors the condensation of GS and $G_2S$ into oligomers, i.e., is linked to the establishment of cross-strand bonds (*22*). Following these rapid changes in fluorescence and light scattering, complex slower changes were observed as follows.

(1) The intensity of light scattering displayed a short lag followed by an increase up to a plateau, reached within 5 min.

(2) Pyrenyl-actin fluorescence displayed a short lag followed by a decrease to almost the same value as the fluorescence of G-actin, then a slower increase to a final plateau in which the fluorescence was 5-fold higher than that of pyrenyl-G-actin. Figure 4b further shows that the lag and decrease in pyrenyl-actin fluorescence temporally coincided with the lag and increase in light scattering. The subsequent slower increase in pyrenyl actin fluorescence took place in large part on assembled F-actin−$S_1$. The rate of the slow fluorescence increase appeared minimally sensitive to the rate of polymerization (data not shown).

(3) NBD-actin fluorescence (dashed line in Figure 4a) displayed a modest decrease, then an increase to a plateau value representing the fluorescence of NBD-F-actin−$S_1$, which was 2.9-fold higher than that of NBD-G-actin. The increase in NBD fluorescence occurred on a time scale temporally consistent with the polymerization process, while the increase in pyrene fluorescence was much slower. Hence, the two probes report different elementary steps in the polymerization process.

To get a deeper insight into the nature of the reactions occurring during the NBD fluorescence time course, a series of identical samples containing 2 $\mu$M NBD-labeled CaATP−G-actin were supplemented with 3 $\mu$M $S_1(A_1)$ at time zero, and the time course of NBD fluorescence was monitored. Each sample was rapidly diluted 8-fold at different times of the assembly process, and NBD fluorescence was measured immediately after dilution. The dilution factor was chosen such that the concentrations of actin and $S_1(A_1)$ after dilution was below the threshold required for oligomer formation (*10*). The value of NBD-actin fluorescence measured after dilution was then multiplied by the dilution factor. The resulting calculated NBD fluorescence (open squares in Figure 4a) represents exactly the contribution, in the original

fluorescence measurement before dilution (dashed line in Figure 4a), of the species that have assembled in an irreversible fashion, i.e., which do not dissociate upon dilution. The contribution of the fluorescence of oligomers that are in rapid equilibrium with G-actin and $S_1$ is therefore eliminated. A reconstituted time course of NBD fluorescence strictly linked to the formation of F-actin$-S_1$ was therefore generated point by point (open squares), each sample diluted at time $t$ providing one data point. The curve described by the open squares started from a value of NBD fluorescence equal to the fluorescence of G-actin or of GS and $G_2S$ complexes (equal to 1 by convention) and superimposed the original fluorescence curve before dilution (dashed line) in the very late stages of assembly. The curve described by open squares perfectly superimposed the time course of increase in light scattering, once the extent of change was normalized between 0 and 1 for the two curves. This result indicated that the observed time course of NBD fluorescence (dashed line in Figure 4a) was the sum of several components, one of which is shown in the inset to Figure 4a, the other representing the formation of F-actin$-S_1$. The fact that NBD fluorescence first decreases then increases, indicates that a simple reaction A $\rightarrow$ B, in which B would be the F-actin$-S_1$ final product, is inadequate, and at least two consecutive steps are involved in the fluorescence change. A tentative A $\rightarrow$ B $\rightarrow$ C scheme was proposed to analyze light scattering and fluorescence data. The observed NBD fluorescence can be described by the following equation:

$$F_{obs} = [A]f_1 + [B]f_2 + [C]f_3 \quad (1)$$

with

$$[A_o] = [A] + [B] + [C] \quad (2)$$

in which $f_1$, $f_2$, and $f_3$ represent the specific fluorescences of the species A, B, and C, respectively, and $[A_o]$ is the total actin concentration. For simplicity, we assume that only species A (oligomers) is present at time zero, B is a kinetic intermediate, and C is F-actin$-S_1$. The molecular nature of the reactions described by A $\rightarrow$ B and B $\rightarrow$ C is not known. Data in Figure 4a indicate that the formation of C from B is described by the change in light scattering. Hence the curve $y(t)$, representing the recorded change in light scattering, varying between 0 and 1, was used to generate the corresponding change in fluorescence due to the formation of $C$, as follows:

$$C = [A_o]\frac{y(t)}{f_3 - f_2} \quad (3)$$

Combining eqs 1, 2, and 3 leads to

$$F_{obs} = f_1[A_o] + (f_1 - f_2)[B] + y[A_o]\frac{f_3 - f_1}{f_3 - f_2} \quad (4)$$

Therefore, the time course of the B intermediate can be derived:

$$[B] = \frac{1}{f_1 - f_2}\left[f_1[A_o] - F_{obs} + [A_o]y\frac{f_3 - f_1}{f_3 - f_2}\right] \quad (5)$$

The time courses of [B] can be compared at different total concentrations $[A_o]$ using the molar fraction of B, $r_B = [B]/[A_o]$, as follows:

$$r_B = \frac{1}{(f_1 - f_2)}\left[f_1 - \frac{F_{obs}}{[A_o]} + y\frac{f_3 - f_1}{f_3 - f_2}\right] \quad (6)$$

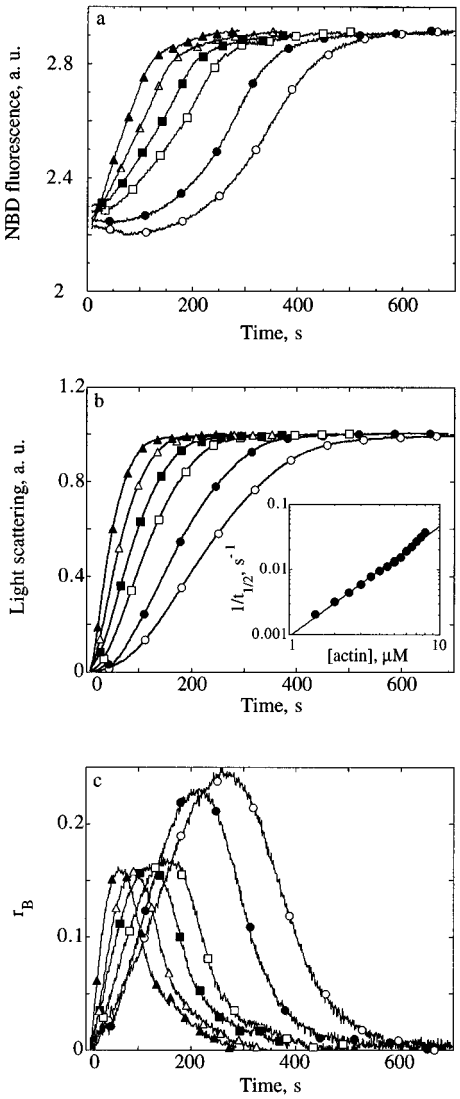


FIGURE 5: Evidence for at least two consecutive steps in the pathway of assembly of F-actin$-S_1$ from G-actin$-S_1$ oligomers. CaATP$-$G-actin (44% NBD-labeled) was polymerized at the following concentrations (in micromolar). (○) 2.5; (●) 3; (□) 4; (■) 5; (△) 6; (▲) 7. NBD fluorescence (panel a) and light scattering intensity at 475 nm (panel b) were recorded simultaneously. The NBD fluorescence scale is adjusted so that the fluorescence of G-actin is 1 for each sample. The change in light scattering is normalized to 1 for each sample. The inset in panel b is a logarithmic plot of the dependence of the half-polymerization time versus actin concentration. Panel c represents the time course of the molar fraction $r_B$ of intermediate B as defined by eq 6.

Assuming that the specific NBD fluorescence of G-actin, GS, and $G_2S$ complexes is $f_o = 1$ by convention, experimental data indicate that the specific fluorescence of oligomers, $f_1$, is 2.1, and the specific fluorescence of F-actin$-S_1$, $f_3$, is 2.9. The value of $f_2$ cannot be determined experimentally with high accuracy, but in experiments carried out at low actin concentration (1.5$-$3 $\mu$M), the decrease in NBD fluorescence linked to the A $\rightarrow$ B process was large enough to provide a rough plausible estimate of $f_2 = 1$ (Table 1).

Figure 5 shows the simultaneous recordings of the changes in light scattering and NBD fluorescence at a series of actin

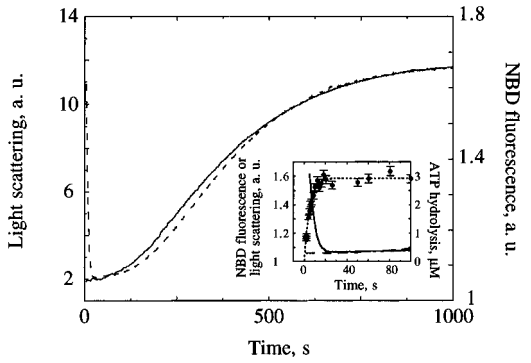


FIGURE 6: Simultaneous changes in light scattering and NBD-actin fluorescence during assembly of Mg-G-actin−$S_1$. MgATP−G-actin (3 $\mu$M, 80% NBD-labeled) was combined with 4.5 $\mu$M $S_1$($A_1$). Changes in light scattering (solid line) and NBD fluorescence (dashed line) were recorded on parallel samples. (Inset) Correlation between the initial decrease in NBD fluorescence and the chemical cleavage of actin-bound ATP (●).

concentrations in the presence of saturating amounts of $S_1$-($A_1$) and the time course of $r_B$ derived from these data using eq 6.

The rate of F-actin−$S_1$ assembly varied very cooperatively with actin concentration at saturating amounts of $S_1$. The logarithmic plot of $t_{1/2}$ vs (actin) displayed a slope of 3, indicating that the association of three molecules of actin-containing species is involved in the overall reaction (Figure 5b, inset). The actin concentration dependence of $r_B(t)$ displayed in Figure 5c indicates that, although the formation of B was slower at lower actin concentration, the maximum molar fraction of B transiently formed was higher.

The changes in pyrenyl- and NBD-actin fluorescences associated with the polymerization of MgATP−G-actin induced by $S_1$ were qualitatively similar to those recorded for CaATP-actin assembly (Figure 6). The initial decrease in NBD fluorescence preceding the formation of F-actin−$S_1$ was much faster than for Ca-actin. As a result, most of the subsequent increase in NBD fluorescence superimposed the light scattering curve.

*ATP Hydrolysis and $P_i$ Release Associated to the Assembly of F-Actin−$S_1$.* Hydrolysis of ATP associated with salt-induced polymerization of actin occurs on F-actin, in two consecutive steps, chemical cleavage of the $\gamma$-phosphoester bond followed by the slower release of $P_i$ (*13*, *15*, *16*).

When CaATP−G-actin 1:1 complex was polymerized into F-actin−$S_1$, the cleavage of the $\gamma$-phosphate of ATP was clearly largely uncoupled from the polymerization reaction (Figure 7a). The rate constant for ATP hydrolysis on F-actin−$S_1$ was 0.009 $s^{-1}$, a value very similar to the one found for ATP hydrolysis in polymerization of CaATP-actin into filaments (*17*, *18*). The increase in pyrenyl-actin fluorescence was a slower process subsequent to cleavage of the $\gamma$-phosphate of ATP.

The release of $P_i$ was monitored using the MESG/guanosine phosphorylase linked enzyme assay (*13*). Data displayed in figure 7a show that the increase in absorbance at 360 nm, which monitored $P_i$ release, closely superimposed the slow increase in pyrenyl fluorescence. The rate constant for $P_i$ release was 0.006 $s^{-1}$. In conclusion, in the assembly of F-actin−$S_1$ from CaATP−G-actin, ATP hydrolysis and $P_i$ release both are slow processes uncoupled from the polymerization reaction. The fluorescence of pyrenyl-actin, which is 4-fold higher in the rapidly formed G-actin−$S_1$ oligomers (*10*) than in the G-actin state, was quenched, upon formation of F-ADP-Pi-actin−$S_1$, to the level of G-actin and increased again to a 6-fold higher value upon $P_i$ release (Table 1). Therefore, when $S_1$ is bound to F-actin, the fluorescence of pyrenyl-actin is a good probe reporting the structural changes in the filament which are linked to the liberation of $P_i$ in the medium, such as weakening of actin−actin bonds (*19*) and decrease in bending modulus (*20*).

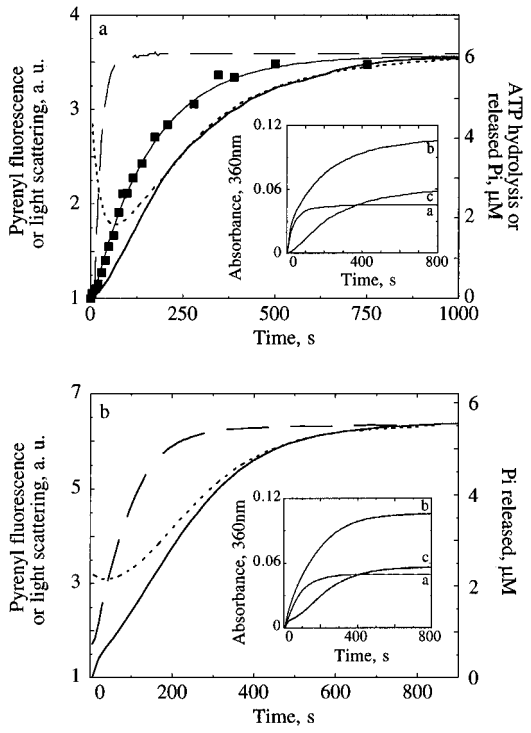


FIGURE 7: ATP hydrolysis and Pi release during F-actin−$S_1$ assembly. (A) Ca-actin. $\gamma$-($^{32}$P)-labeled Ca-ATP−G-actin (6 $\mu$M, 81% pyrenyl-labeled) was polymerized by addition of 9 $\mu$M $S_1$-($A_1$) at time zero. The time courses of changes in light scattering at 600 nm (dashed line), pyrenyl-actin fluorescence (dotted line) and cleavage of ATP (■) were monitored. Cumulated data points for ATP hydrolysis from two identical experiments are displayed. The release of inorganic phosphate ($P_i$) was monitored using the MESG/pyrophosphorylase enzyme-linked assay (solid line). The fluorescence, light scattering, and $P_i$ ordinate scales have been adjusted so that the final values coincide with the final amount of released $P_i$ (6 $\mu$M). The fluorescence and light scattering of pyrenyl G-actin are subtracted. (Inset) Raw absorbance data for the $P_i$ assay. Curve a is the time course of absorbance change at 360 nm recorded in the absence of enzyme or MESG, which reflects the turbidity developed by the polymerization of 6 $\mu$M F-actin−$S_1$. Curve b is the recorded absorbance change in the presence of MESG + enzyme, which reflects the summed contributions of the polymerization and $P_i$ measurement. Curve c represents the difference b − a, i.e., the time course of $P_i$ release (solid line in main frame). (B) Mg-actin. Conditions and analysis are as described under panel a.

When MgATP−G-actin complex was assembled into F-actin−$S_1$, ATP hydrolysis and $P_i$ release occurred on very different time scales.

Chemical cleavage of ATP temporally correlated with the rapid decrease in NBD fluorescence that preceded the increase in light scattering reporting formation of decorated filaments (*22*). Decorated filaments therefore were assembled from MgADP-$P_i$ actin−$S_1$ oligomers.

The time course of $P_i$ release occurred slowly on the assembled filaments and again temporally correlated with the increase in pyrenyl-actin fluorescence (Figure 7b) with a rate constant of 0.006 $s^{-1}$, very similar to the rate of $P_i$ release in Mg-F-actin assembly (*13*).

Scheme 1

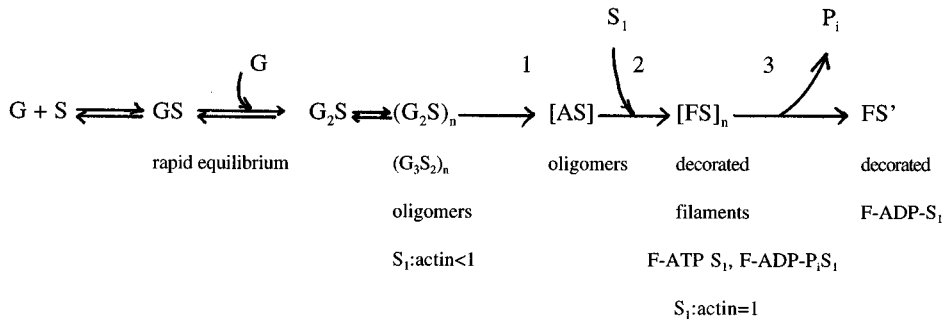


*Kinetic Model for $S_1$-Induced Polymerization of G-Actin into F-Actin−$S_1$.* The experiments described above show that the assembly of F-actin−$S_1$ can be described by a sequence of elementary steps, following the rapid formation of G-actin−$S_1$ oligomers. A minimum number of two kinetic steps is required to account for the lag preceding the increase in light scattering or the decrease in pyrenyl fluorescence. The following Scheme 1 was tentatively proposed to account for the experimental kinetic curves.

Step 1 represents the isomerization of the $G_4S_2$ and $G_3S_2$ oligomeric species into a AS oligomer. No change in light scattering nor pyrenyl fluorescence is associated to this step, but NBD fluorescence is lower in AS than in $(G_2S)_n$. On Mg-actin, ATP hydrolysis is associated to this step.

Step 2 is the condensation of AS oligomers into F-actin−$S_1$ with concomittant binding of $S_1$. This step is associated to a large increase in light scattering, an increase in NBD-actin fluorescence, and a large decrease in pyrenyl-actin fluorescence. The associated binding of $S_1$ to sites made available by the condensation causes a very large increase in stability of the polymer, thus making the polymerization process irreversible.

Step 3 is the $P_i$ release step, which is a first-order process taking place on F-actin−$S_1$, and is linked to an increase in pyrenyl-actin fluorescence.

## DISCUSSION

The mechanism of $S_1$-induced polymerization of ATP−G-actin into F-actin−$S_1$ decorated filaments appears different from the salt-induced spontaneous assembly of G-actin into F-actin. G-actin and $S_1$ associate rapidly into small complexes that further condense into oligomeric species of increasing size and stability. The initially formed GS and $G_2S$ complexes first condense rapidly into short oligomers that have a relatively low stability ($K \cong 10^6$ $M^{-1}$) and contain $S_1$ and actin in a molar ratio lower than 1. Subsequent binding of $S_1$ to available sites occurs as further condensation into large F-actin−$S_1$ structures takes place. This last step of the assembly reaction is irreversible, i.e., increasing the $S_1$:actin molar ratio up to 1 as decorated filaments are formed results in a large increase in stability of the polymer. Upon addition of at least 1 M equiv $S_1$ to G-actin, all actin molecules eventually incorporate into F-actin−$S_1$ filaments. At the end of the reaction, no monomer−polymer exchange reactions occur, i.e., no monomer critical concentration can be detected. The kinetics of F-actin−$S_1$ assembly cannot be described by a simple nucleation-growth process, because the rate constant for association of G-actin−$S_1$ complexes to filament ends is relatively low and of the same order of magnitude as the rate constant for end-to-end annealing of short polymers. Hence, both processes contribute to the assembly of F-actin−$S_1$. This major difference with salt-induced assembly of F-actin is due to the fact that $S_1$ strongly enhances the formation of G-actin−$S_1$ oligomers, thus lowering the free energy for nucleation. The same feature was observed when actin was polymerized at very high concentration (*21*).

The proposed kinetic scheme within which actin−$S_1$ oligomers having an actin:$S_1$ content higher than 1 are directly involved in the pathway leading to F-actin−$S_1$ is supported by several observations: (i) the threshold concentration at which spontaneous assembly of F-actin−$S_1$ takes place corresponds to the concentration at which oligomers are formed; (ii) when $S_1$ is maintained at a constant concentration, the rate of increase in light scattering reached a limit at an actin:$S_1$ molar ratio of 2. This observation indicates that condensation of GS and $G_2S$ into oligomeric species in which energetically unfavorable lateral actin−actin bonds are formed is a prerequisite to the subsequent binding of $S_1$ to new sites made available by condensation. (iii) When actin is maintained at a constant concentration, the dependence of the rate of assembly on $S_1$ concentration shows a saturation behavior also consistent with a maximum rate of polymerization reached at an $S_1$-actin molar ratio of about 0.5.

The present data demonstrate that the kinetics of ATP hydrolysis and $P_i$ release in the medium are very similar in salt-induced and $S_1$-induced assembly of Ca-actin. Both reactions occur slowly on the polymer, in a fashion uncoupled from polymerization. In the case of Mg-actin, however, ATP hydrolysis precedes the assembly of decorated filaments and occurs rapidly on oligomer precursors (*22*). Release of $P_i$ in contrast, occurs slowly on Mg-F-actin−$S_1$, at the same rate as on Mg-F-actin. We conclude that the rate of the conformational change of F-actin, which kinetically limits the release of $P_i$, is not affected by the binding of $S_1$ to F-actin.

The kinetic analysis of the simultaneous changes in light scattering and fluorescence of pyrenyl- and NBD-labeled actin has allowed us to propose a minimum number of elementary steps and kinetic intermediates in the assembly of F-actin−$S_1$, because each probe reacts in its own specific fashion to structural changes associated with the different steps. A decrease in NBD-actin fluorescence, but no change in pyrenyl-actin fluorescence nor in light scattering is associated with the formation of $(AS)_n$; pyrenyl-actin fluorescence decreases, while NBD-actin fluorescence and light scattering both increase during formation of F-actin−$S_1$; finally only pyrenyl-actin fluorescence is highly sensitive to the release of $P_i$. This result is in agreement with previous

observations made when polymerization of actin was induced by salt (*18*).

## REFERENCES


1. Cooke, R., and Morales, M. F. (1971) *J. Mol. Biol. 60*, 249−261.
2. Yazawa, Y., and Yagi, K. (1973) *J. Biochem. (Tokyo) 73*, 567−580.
3. Grazi, E., Ferri, A., Lanzara, V., Magri, E., and Zaccarini, M. (1980) *FEBS Lett. 112*, 67−69.
4. Detmers, P., Weber, A., Elzinga, M., and Stephens, R. E. (1981) *J. Biol. Chem. 256*, 99−105.
5. Miller, L., Philips, M., and Reisler, E. (1988) *J. Biol. Chem. 263*, 1996−2002.
6. Chen, T., and Reisler, E. (1991) *Biochemistry 30*, 4546−4552.
7. Lheureux, K., Forné, T., and Chaussepied, P. (1993) *Biochemistry 32*, 10005−10014.
8. Valentin-Ranc, C., Combeau, C., Carlier, M.-F., and Pantaloni, D. (1991) *J. Biol. Chem. 266*, 17871−17879.
9. Blanchoin, L., Fievez, S., Travers, F., Carlier, M.-F., and Pantaloni, D. (1995) *J. Biol. Chem. 270*, 7125−7133.
10. Valentin-Ranc, C., and Carlier, M.-F. (1992) *J. Biol. Chem. 267*, 21543−21550.
11. Carlier, M.-F., Pantaloni, D., and Korn, E. D. (1987) *J. Biol. Chem. 262*, 3052−3059.
12. Webb, M. R. (1992) *Proc. Natl. Acad. Sci. U.S.A. 89*, 4884−4887.
13. Melki, R., Fievez, S., and Carlier, M.-F. (1996) *Biochemistry 35*, 12038−12045.
14. Hill, T. L. (1987) *Linear Aggregation in Cell Biology*, Chapter 1, p 6, Springer-Verlag, New York.
15. Carlier, M.-F., and Pantaloni, D. (1986) *Biochemistry 25*, 7789−7792.
16. Combeau, C., and Carlier, M.-F. (1988) *J. Biol. Chem. 263*, 17429−17436.
17. Pollard, T. D., and Weeds, A. G. (1984) *FEBS Lett. 170*, 94−98.
18. Carlier, M.-F., Pantaloni, D., and Korn, E. D. (1984) *J. Biol. Chem. 259*, 9983−9986.
19. Carlier, M.-F. (1991) *J. Biol. Chem. 266*, 1−4.
20. Isambert, H., Venier, P., Maggs, A. C., Fattoum, A., Kassab, R., Pantaloni, D., and Carlier, M.-F. (1995) *J. Biol. Chem. 270*, 11437−11444.
21. Matsudaira, P., Bordas, J., and Koch, M. H. (1987) *Proc. Natl. Acad. Sci. U.S.A. 84*, 3151−3155.
22. Fievez, S., Pantaloni, D., and Carlin, M.-F. (1997) *Biochemistry 36*, 11837−11842.


BI971206O